

## Removal of Phenolics from Wastewater by Fe<sub>2</sub>O<sub>3</sub> Impregnated Sawdust as Adsorbent: Adsorption Isotherm and Kinetic Studies

Arunima Nayak, Brij Bhushan, Vartika Gupta\*

Department of Chemistry,  
Graphic Era (Deemed to be University), Dehradun, Uttarakhand, India.

\*Corresponding author: vartikagarggurukul15@gmail.com

(Received April 17, 2019; Accepted October 1, 2019)

### Abstract

In this study, magnetic nanoparticles (MNPSD) from abundantly available lignocellulosic waste viz. sawdust was successfully synthesized via co-precipitation method and consequently used for the removal of model phenolics (Catechol and Resorcinol) from aqueous solution under batch mode method. Batch adsorption studies revealed irrespective of adsorbate types, higher sorption of such phenolics occurring at acidic pH (pH=3), contact time of 60mins and at 25°C. The results obtained from pH studies indicates that electrostatic interaction may be responsible for the binding of Catechol and Resorcinol onto MNPSD, while film or particle diffusion mechanisms to be operative during the transfer of such phenolics from the liquid phase. The isotherm outcomes demonstrated that irrespective of adsorbate types, Langmuir model was operative over the studied phenolics concentration and kinetics data followed pseudo-second-order model over the entire time frame. Thus, the experimental results reveal the usefulness of MNPSD as a suitable Nano adsorbent for wastewater treatment.

**Keywords-** Sawdust, Magnetic Nano Adsorbent, Phenolic Compounds, Adsorption Isotherm, Adsorption Kinetics.

### 1. Introduction

Industrial wastewater is often containing diverse types of organic contaminants, which constitute a major source of water pollution (Mu'azu et al., 2017). Among them, phenol and their substituent are supposed to be one of the major organic pollutants as they have high toxicity and carcinogenicity (Issabayeva et al., 2018). The widespread use of such organic compounds in many petrochemical and chemical industries, pharmaceutical and resin manufacturing industries has resulted in their extensive presence in wastewaters (Kurnik et al., 2015). The discharge of such industrial waste effluent into water bodies affects the water eco-system as well as devastates the aesthetic nature of environment (Mittal et al., 2009). Also, phenolic compounds impart nasty odor and unpleasant taste to fresh water which makes it totally unfit/or unusable for human consumption (Kumar et al., 2011). Because of their bioaccumulation and stability, phenolic compounds are resistant to biodegradation and are difficult to be eliminated. Thus, the European Environmental Agency (EEA) and the United States Environmental Protection Agency (USEPA) have enlisted phenolic compounds on the priority contaminants list (Villegas et al., 2016). According to the World Health Organization (WHO), the allowable limit of phenolic compounds in potable water is set 0.001mg/L. As a

consequence, it is essential to remove phenolics from wastewater up to their permissible limit prior to release in water bodies (Gracioso et al., 2019). Two model phenolic compounds- Catechol and Resorcinol were selected for the study.

A variety of wastewater treatment technologies have been adopted in the past decades but are not efficient to remove organic compounds (Gupta et al., 2015). Among the available treatment methods, adsorption has been proposed as the most reliable and a superior technology as compared to other methods (Ahmad and Danish, 2018; Zhao et al., 2017). Activated carbons (ACs) have been extensively used as adsorbent due to their surface properties like extensive surface area, porosity and favorable surface characteristics (Sharma et al., 2017). But, commercial activated carbons are not cost-efficient due to the high cost of its precursor like coal, wood, peat and petroleum residues.

In this respect, the use of lignocellulosic wastes/biomasses as an alternative adsorbent is not only cost-efficient but is highly effective to remove diverse pollutants from wastewater due to the fact that they are abundantly available, eco-friendly; biodegradable and favorable surface chemistry (Bayat et al., 2015). Various lignocellulosic-based agricultural residues/biomass (wheat bran, rice husk, tree barks, fruits and vegetables peels and sawdust) have been reported as potential biosorbents (Kataria and Garg, 2018). Among these, sawdust due to its abundant availability as solid biomass from the lumber mills as well as its high fraction of lignocellulose could be used as a low-cost precursor for the production of quality adsorbent (Chen et al., 2018). However, some literature has shown that sawdust in its raw form exhibited lower removal efficiency and showed other disadvantages such as discharge of color, polyphenols and tannins, which associated with secondary pollution load in water bodies (Nayak et al., 2017). Therefore, the sorption efficiencies of such lignocellulosic wastes/or residues can be improved by various physical/ or chemical activation methods but these methods usually require higher temperature, longer activation time and chemical consumption thus are not acceptable.

In this regard, nanotechnology has emerged as an attractive area of study and has created much attention in the field of environmental remediation, pollution detection and pollutant adsorption (Gupta and Nayak, 2012). Iron-oxide Nano adsorbent is known to demonstrate potential adsorption efficiency on account of its large surface area, high porosity and Nano-scale particle size (Jain et al., 2018). In addition, it could be efficiently separated from liquid phase by using a permanent magnetic. (Jain et al., 2018). Thus, the present study has focused on synthesizing iron-oxide Nano adsorbent from sawdust (MNPSD) so as to assess its adsorptive behavior via physicochemical characterization as well as batch adsorption studies. This study was made not only to determine the adsorptive behavior of MNPSD, but also the likely parameters that affected the sorption process were assessed.

## 2. Materials and Methods

### 2.1 Chemicals and Reagents

Model phenolics: Catechol and Resorcinol (of technical grade and 98% purity) were received from M/S Merck, India. Physicochemical and toxicological properties of Catechol and Resorcinol are shown in Table-1. The stock/working sample solutions of all phenolics were made with de-ionized water.

### 2.2 Development of Magnetic Nano Adsorbent

The preparation of magnetic nanoparticles impregnated with sawdust was performed as describe in our earlier work (Nayak et al., 2017).

### 2.3 Characterization of the Adsorbents

Field emission scanning electron microscope (Fe-SEM) with EDX analysis (Leo Elektronemikroskopie GmbH, Germany) was made to examine the textural characteristics and elemental composition of adsorbents. AUV-Visible spectrophotometer (UV10 HEDM218008, Thermo scientific) was used to evaluate the equilibrium concentration of studied model phenolics. The presence of surface functionalities on adsorbent was evaluated by Fourier transform infrared spectra (model: Elmer-1600 spectrophotometer, USA). Transmission Electron Microscope (TEM) (model: FEITECNAI G2 microscope) study was performed to analyze the particle structure and size. Vibrating sample magnetometer analysis (VSM) was made to determine the magnetic characteristics of the nanoparticles (Model 155, Princeton Applied Research) at room temperature.

The surface basicity, acidity and  $\text{pH}_{\text{pzc}}$  of RSD and MNPSD were evaluated by the methodology as reported in previous study (Nayak et al., 2017).

### 2.4 Adsorption Isotherm and Kinetic Studies

For both batch isotherm and kinetic studies, a fixed amount of adsorbent (0.1g) was contacted with a series of 100mL solution of Catechol and Resorcinol solution of different initial concentrations (2.5-50 mg/L) and adjusted at a fixed pH with 0.1M NaOH/or  $\text{HNO}_3$ . The flasks were placed under agitation for 180mins at 100 rpm and at 25°C. The sample solutions were taken out at an appropriate period of time and filtered. The concentration of phenolics that remained in reaction medium was calculated spectro photo metrically using UV-Visible at 275nm for Catechol and 273nm for Resorcinol, respectively.

The maximum uptake efficiency ( $q_e$ , mg/g) was evaluated as:

$$q_e = (C_o - C_e) \frac{V}{W} \quad (1)$$

where,  $q_e$  is the amount of phenolics adsorbed per gram of adsorbent (mg/g),  $C_o$  is the initial concentration of phenolics and  $C_e$  is the final concentration (mg/L).  $W$  is the weight of adsorbent (g) and  $V$  is the volume of solution (L).

### 3. Results and Discussion

#### 3.1 Characterization Studies of Adsorbents

The FTIR study of MNPSD (Figure 1a) indicates the prominent and broad peak at  $3500\text{-}3200\text{cm}^{-1}$  (O-H stretch),  $1569\text{cm}^{-1}$  (carboxylate, C=O stretch),  $1633$  and  $1413\text{cm}^{-1}$  (carboxyl C-O stretch),  $1124$  and  $1020\text{cm}^{-1}$  (C-OH stretch). The new peak is observed at around  $557\text{cm}^{-1}$  in MNPSD indicating the presence of Fe-O group onto its surface.

On the other hand, the FTIR spectrum of MNPSD loaded with Catechol (Figure 1b), revealed the shifting and disappearance of some absorption peak frequencies that were mainly corresponding to carboxylic, phenolic and hydroxyl groups. Significant shifting of some absorption peak frequencies from  $3418$  to  $3449$ ,  $1636$  to  $1628$ ,  $1413$  to  $1411$ ,  $1124$  to  $1132$ , and  $638$  to  $643\text{cm}^{-1}$  was observed on MNPSD after adsorption of Catechol.

Similar observations were made for the FTIR spectra of MNPSD loaded with Resorcinol (Figure 1c). Significant shifting of some absorption peak frequencies from  $3418$  to  $3441$ ,  $1636$  to  $1622$ ,  $1413$  to  $1416$ ,  $1124$  to  $1139$ , and  $638$  to  $635\text{cm}^{-1}$  was observed on MNPSD after adsorption of Resorcinol. FTIR studies thereby revealed the successful binding of the adsorbates onto MNPSD.

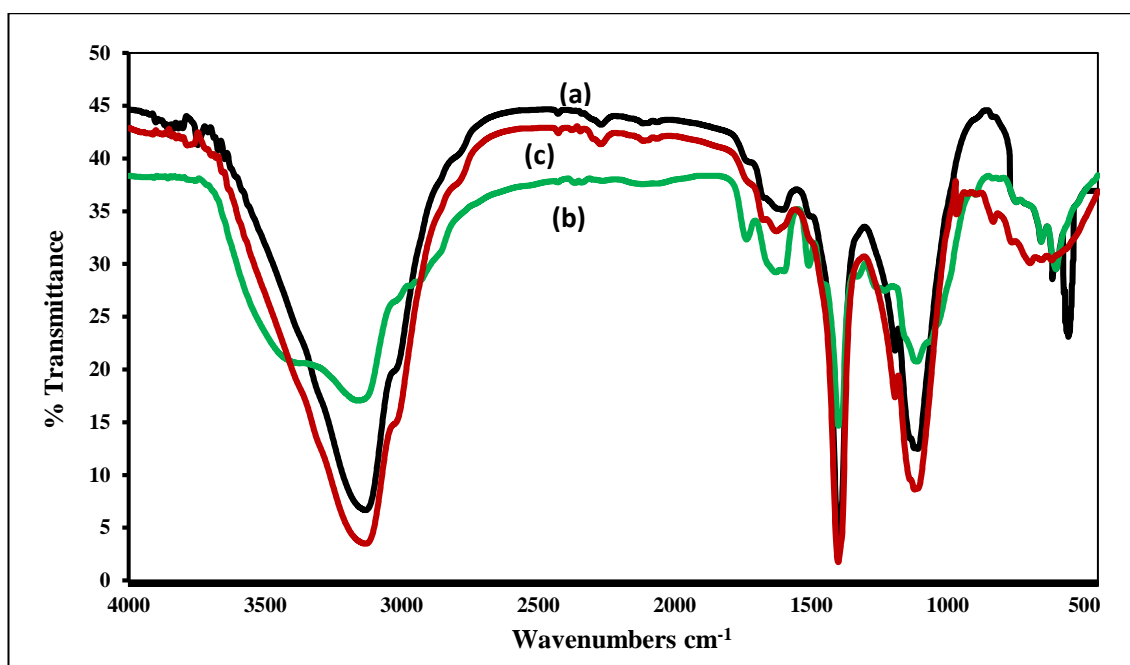
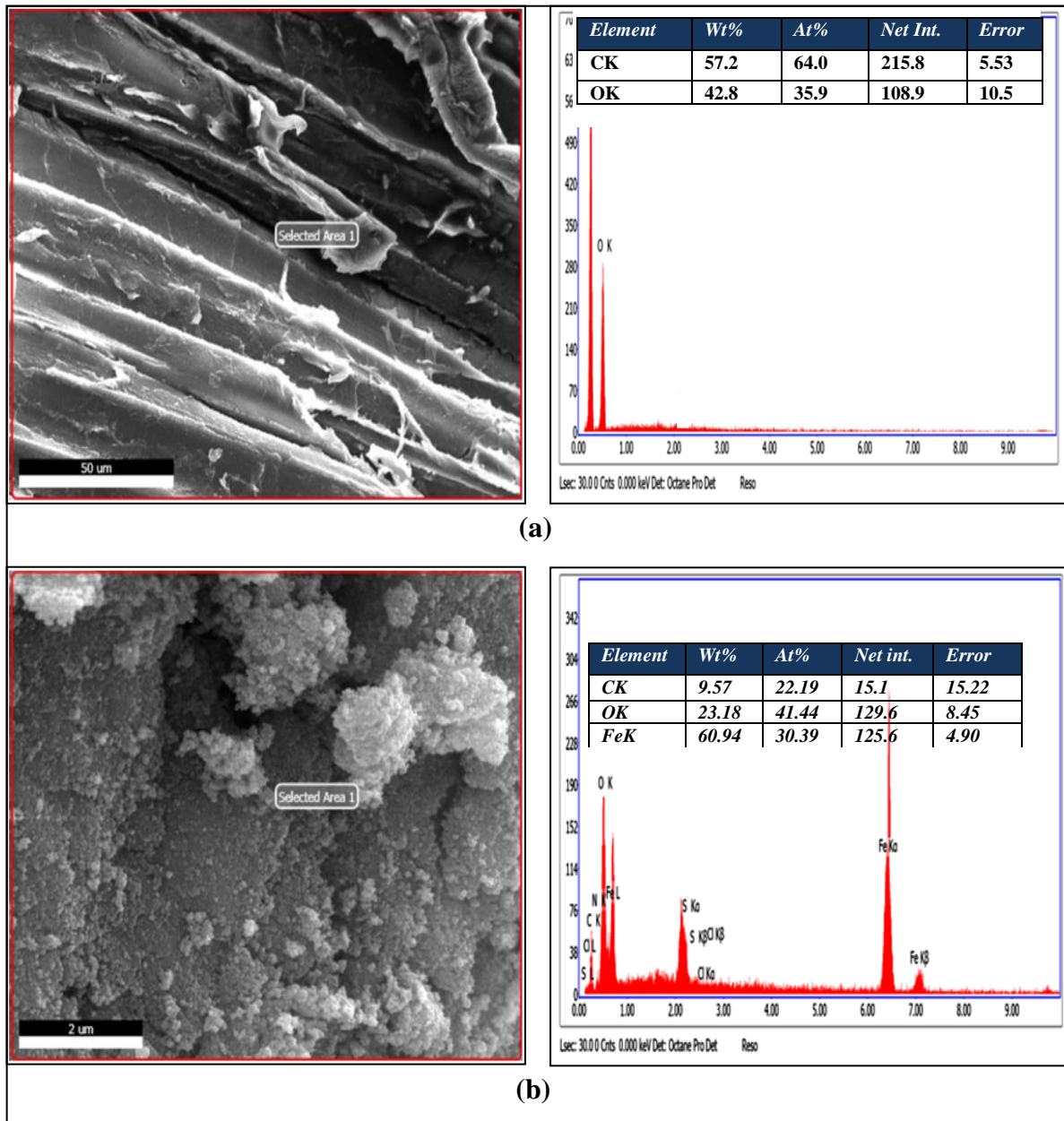


Figure 1. FTIR spectra of (a) MNPSD; (b) MNPSD after adsorption of catechol; (c) MNPSD after adsorption of resorcinol

Fe-SEM image of RSD (Figure 2a) reveals the absence of porosity on RSD (Figure 2a), while the image of MNPSD (Figure 2b) reveals that the particles of MNPSD were agglomerated thus, making its surface coarse and rough (Jain et al., 2018).

EDX study was made to determine the elemental composition of RSD and MNPSD (Figure 2a, b). It is clear from the EDX data of RSD (Figure 2a) the weight percent (%) of carbon and oxygen is 57.2 and 42.8%, respectively. In the case of MNPSD (Figure 2b), the weight percent (%) of Fe is about 60.9% and that of carbon is only 9.57%, which reveals the presence of iron-oxide nanoparticles onto MNPSD surface.



**Figure 2. SEM micrographs and EDX of (a) RSD; (b) MNPSD**

TEM micrographs of synthesized MNPSD are shown in Figure 3 (a, b). The resulting micrograph of MNPSD as shown in Figure 3(a) reveals the mono-dispersed, compact and

spherical nature of the particles. Particle size was in the range of 22-23 nm; thereby demonstrating its Nano-sized nature (Figure 3).

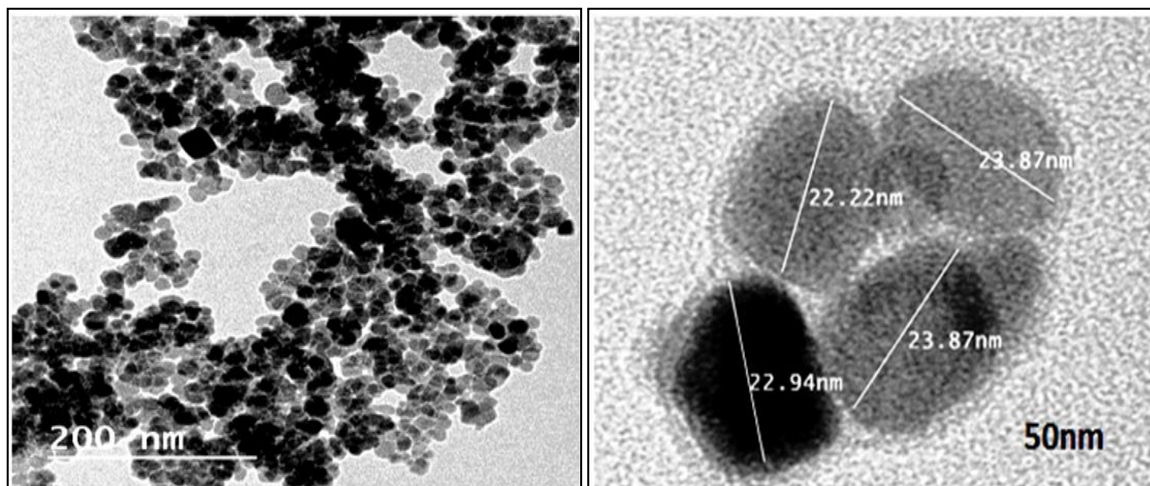


Figure 3. TEM micrographs of MNPSD

The magnetic behavior of the MNPSD was evaluated by VSM studies. Figure 4 showed the presence of a magnetic hysteresis loop which reveals its superparamagnetic characteristic. A similar investigation was proposed by Soares et al., 2016.

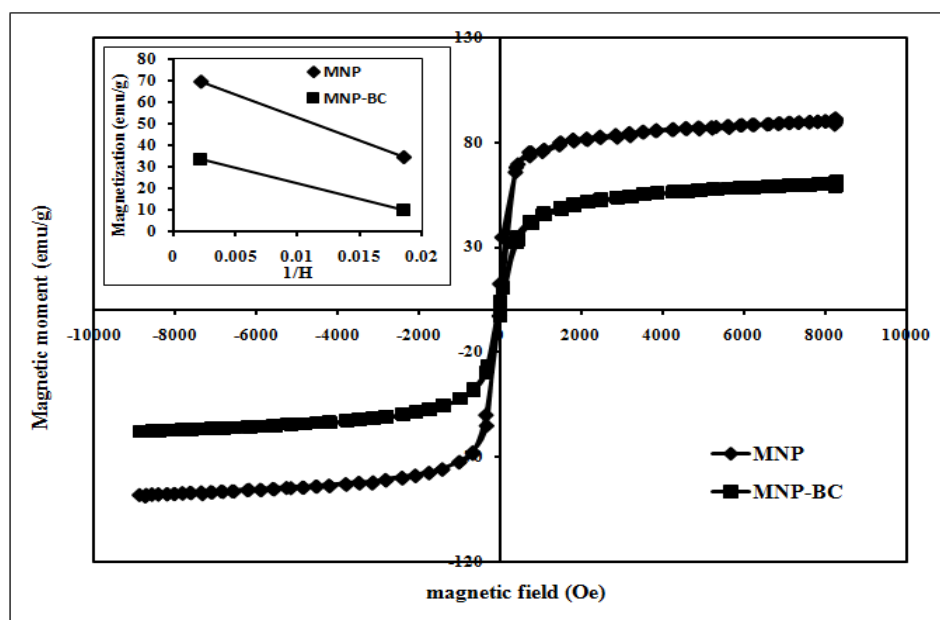


Figure 4. Vibrating sample magnetometer (VSM) of MNPSD

The  $pH_{pzc}$  values of MNPSD and RSD were found to be about 4.11 and 5.0. The analysis of acidic and basic surface functionalities on both adsorbents as calculated from the titration experiments are shown in Table 1.

**Table 1. Surface acidity/basicity and  $pH_{pzc}$  analysis**

Adsorbent	Total acidic groups (mEq/g)	Total basic groups (mEq/g)	Total groups (mEq/g)	$pH_{pzc}$
MNPSD	1100	1000	2100	4.11
RSD	1300	1100	2400	5.0

### 3.2 Batch Adsorption Studies

#### 3.2.1 Effect of PH and Underlying Mechanism During Adsorption

Solution pH is considered an important parameter as it poses a significant influence on ionization/or dissociation of phenolic compounds and the surface charge of MNPSD (Cui et al., 2019; Nono et al., 2016). The pH study conducted on MNPSD for uptake of phenolics was studied with fixed adsorbent dosage of 1g/L, at fixed initial concentration (50 mg/L) but under different pH of 2-9. The outcomes are shown in Figs.5a, b. Results revealed that the removal efficiency (mg/g) of MNPSD for phenolics was observed to be very high under acidic medium (pH=3) and then it showed a gradual decrease with increase in solution pH from 4 to 9. The results obtained from such study can be ascribed on the basis of ionization of phenolics and  $pH_{pzc}$  value of adsorbent (Suresh et al., 2011). Catechol and Resorcinol are weak acids and dissociating into a negatively charged Catecnate and Resorcinate ions and hydronium ion (Lin et al., 2011) as given below.

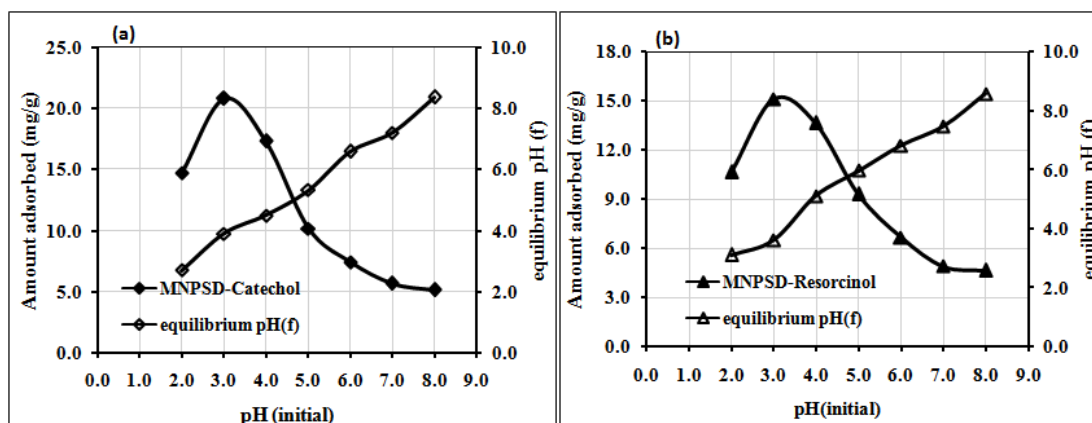


**Figure 5. Effect of solution pH on the uptake of (a) Catechol and (b) Resorcinol onto MNPSD (initial concentration: 50 mg/L; contact time: 60mins; MNPSD dosage: 1 g/L; temperature: 25°C)**



Catechol is abbreviated as Ctc, whereas, Resorcinol is abbreviated as Res.

Under acidic medium, MNPSD surface is positively charged ( $pH < pH_{pzc}$ ;  $pH_{pzc} = 4.11$ ); thereby exhibit a greater efficiency to the molecular or slightly ionized phenolic compounds resulting in increased adsorption capacity (Agarwal and Rani, 2017). While at higher pH ( $pH > pH_{pzc}$ ), MNPSD is deprotonated leading to increase strong repulsion between the

deprotonated MNPSD and the anionic form of phenolics (Catecnate and Resorcinat). Also, irrespective of adsorbate type, the final pH demonstrates a slight difference after the course of adsorption. Therefore, the electrostatic attraction could be responsible for the binding of Catechol and Resorcinol on MNPSD.

**(a) Mechanism for Adsorption of Catechol and Resorcinol onto MNPSD under Acidic Medium**



**(b) Mechanism for Adsorption of Catechol and Resorcinol onto MNPSD under Basic Medium**



Since, the maximum uptake of Catechol and Resorcinol was found under acidic medium (at pH of 3); henceforth, the further tests were carried out at optimum pH for the adsorption of such phenolics onto MNPSD.

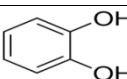
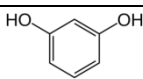
**3.2.2 Effect of Contact Time and Initial Adsorbate Concentration**

The time dependent adsorption tests were conducted on MNPSD at 25°C, at fixed pH of 3, at fixed dosage of 1g/L but under different initial concentrations (20, 30 and 50mg/L). Figs. 6(a, b) illustrated that the sorption of all phenolics were found to be rapid initially (within 60mins) after which the adsorption efficiency steadily decrease to reach equilibrium. Thus, equilibrium contact time selected for MNPSD-phenolics system was 60mins. Initially, a faster uptake rate observed for phenolics onto MNPSD could be due to a well-defined porosity and existence of numerous surfaces active binding sites; there by demonstrating greater uptake efficiency (Shakir et al., 2008). But the decrease in adsorption rate with longer contact time may be attributed to a possible aggregation of adsorbate molecules; thus resulting in resistance to further diffusion.

As the initial concentration of adsorbates increased from 20 to 50 mg/L, the removal efficiency (Q<sub>o</sub>) increased from 16.6 to 21.9mg/g for Catechol and 11.3 to 14.9mg/g for

Resorcinol, respectively. A probable reason for extent of adsorption could be due to that higher adsorbate concentration provide maximum transfer rate of adsorbate towards the adsorbent (Sun et al., 2005). The results further indicate that Catechol has higher binding affinity towards MNPSD as compared to Resorcinol. The difference in the adsorption affinity of such phenolics towards MNPSD may be attributed to several factors like its log-octanol-water partition coefficient (log  $k_{ow}$ ) value, solubility and position of the same functional groups on the benzene ring as has been reported by Sun et al. (2005). Lower solubility and higher log  $k_{ow}$  values for Catechol could be responsible for its higher diffusion and hence higher sorption to MNPSD (Table 2).

**Table 2. Physicochemical properties of catechol and resorcinol**

	<b>Catechol</b>	<b>Resorcinol</b>
Molecular structure		
Molecular Formula	C <sub>6</sub> H <sub>6</sub> O <sub>2</sub>	C <sub>6</sub> H <sub>6</sub> O <sub>2</sub>
IUPAC Name	benzene-1,2-diol	benzene-1,3-diol
Synonyms	Pyrocatechol; Catechol; o-Benzenediol; Pyrocatechine	Resorcin; Resorcinol; m-Benzenediol; Resorzin
Molecular Weight	110.1 g/mol	110.1 g/mol
Solubility in water (25°C)	461 g/L	717 g/L
pK <sub>a</sub>	9.25	9.4
Log octanol-water partition coefficient (log K <sub>ow</sub> )	0.88	0.80
Absorption Maxima (λ <sub>max</sub> )	275 nm	273 nm
Appearance	Colorless crystal, discolor to brown on exposure to light and air	White crystals, discolor to pink on exposure to light and air

### 3.2.3 Adsorption Kinetics

The rate of reaction and kinetics of sorption phenomena were evaluated by the Lagergren's pseudo-first-order and pseudo-second-order kinetic models (Ho and McKay, 1998; Ho et al., 2001). The obtained outcomes were further compared so as to estimate the best-fitted model for studied adsorption system.

The linear pseudo-first-order model is given as:

$$\log (q_e - q_t) = \log k_1 \times \frac{t}{2.303} \quad (10)$$

where  $q_e$  is the adsorption capacity at equilibrium time and  $q_t$ (mg/g) is the amount adsorbed at time  $t$ .  $k_1$  (min<sup>-1</sup>) is the pseudo-first-order rate constants.

The pseudo-second-order kinetic model is given as:

$$\frac{t}{q_t} = \frac{1}{(k_2, q_e^2)} + \frac{t}{q_e} \quad (11)$$

$q_e$  is the equilibrium sorption uptake (mg/g) and  $q_t$  is the amount adsorbed at time  $t$ .  $k_2$ (g/mg/min) is the pseudo-second-order model rate constant.

The model parameter and correlation coefficients of pseudo-first-order and pseudo-second-order model derived from the plots of  $\log q_e - q_t$  versus  $t$  and  $t/q_t$  versus  $t$  and outcomes are illustrated in Table 3. Figure 6 reveal that irrespective of phenolic types, pseudo-second-order model with high regression coefficient ( $R^2$ ) was best fitted to the kinetic data. Also, the theoretical values of uptake capacities (mg/g) for both Catechol and Resorcinol are close to the experimentally derived adsorption capacities; thereby revealed its applicability to describe the adsorption system.

**Table 3. Kinetic parameters for the adsorption of catechol and resorcinol onto MNPSD**

Adsorbent	MNPSD					
Adsorbate concentration	50mg/L	30mg/L	20mg/L	50mg/L	30mg/L	20mg/L
$q_e$ (mg/g) (experimental)	21.9	18.8	17.0	14.9	13.1	11.3
<b>Pseudo-first-order model</b>						
$q_e$ (mg/g) (theoretical)	28.8	15.5	10.5	12.3	9.33	8.94
$k_1$	0.11	0.09	0.07	0.073	0.089	0.062
$R^2$	0.96	0.98	0.95	0.98	0.97	0.98
<b>Pseudo-second-order model</b>						
$q_e$ (mg/g) (theoretical)	22.3	19.2	17.6	15.3	13.8	11.8
$k_2$ (g/mg/min)	0.009	0.011	0.012	0.01	0.013	0.015
$R^2$	0.99	0.99	0.99	0.99	0.99	0.99
<b>Intra-particle diffusion model</b>						
$k_i$	0.51	0.52	0.98	0.53	0.54	0.31
C	19.5	16.7	11.4	10.5	8.70	8.61
$R^2$	0.99	0.99	0.99	0.99	0.99	0.99

### 3.2.4 Adsorption Diffusion Mechanism

In order to investigate the diffusion mechanism of the phenolics towards the MNPSD, Weber and Morris (intra-particle diffusion) model was employed, which is illustrated in Eq. (12) (Weber and Morris, 1963; Akar et al., 2008):

$$q_t = k_i t^{0.5} + C \quad (12)$$

where,  $k_i$ (mg/g/min<sup>0.5</sup>) is the Weber Morris constant and C is the constant related to the thickness of boundary layer.

Figure 6(e, f) indicate the plots of  $q_t$  vs.  $t^{0.5}$  irrespective of adsorbate types, showing three distinct linear regions for both Catechol and Resorcinol: the first straight line shows rapid uptake signifying the immediate adsorption of such phenolics from liquid phase to the MNPSD. The second region shows the rate determining step signifying the gradual sorption stage. The third straight line exhibits the equilibrium adsorption stage of the surface of

MNPSD. Both the second and third region does not pass through the origin, which implies that both film and particle diffusion mechanism may have operated during the diffusion process.

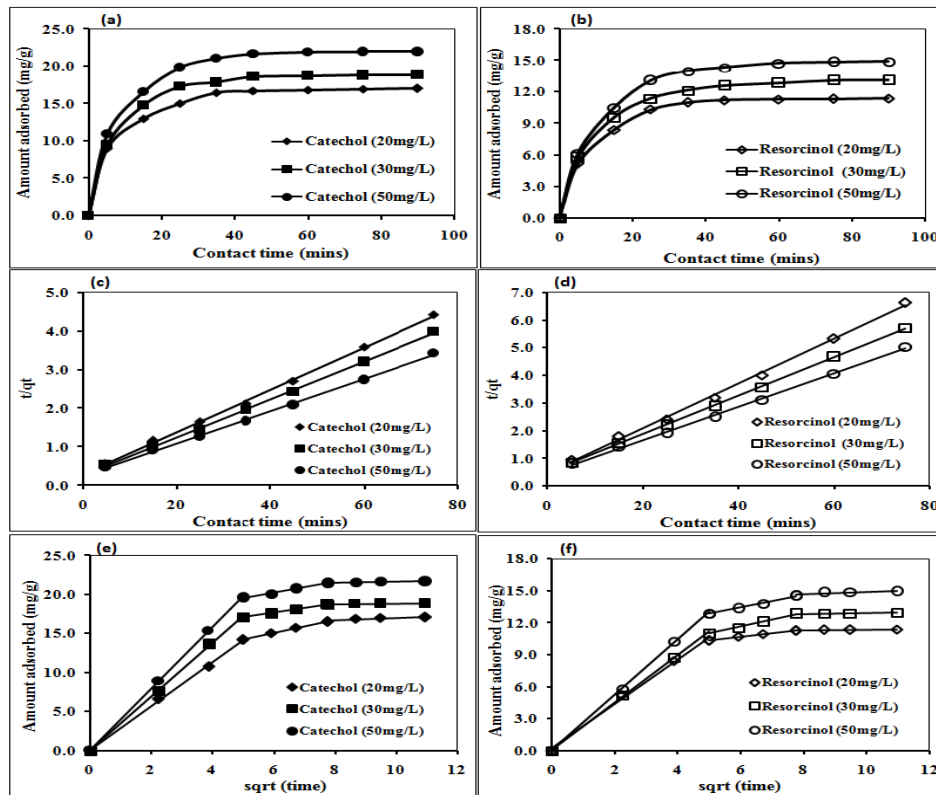


**Figure 6. Results of kinetics of (a) MNPSD-catechol (b) MNPSD-resorcinol applicability of lagergren’s pseudo-second-order model; (c) Applicability of weber Morris plot (initial concentration: 50mg/L; temperature: 25°C; MNPSD dosage: 1 g/L; pH: 3)**

### 3.2.5 Adsorption Isotherm Studies

The results of isotherms of Catechol and Resorcinol onto MNPSD were plotted at fixed pH of 3 and at a fixed temperature of 25°C but under diverse initial concentrations(2.5-50mg/L) and are shown in Figure 7a, b. With an aim to assess the nature of binding mechanism and to understand the sorption process, Langmuir, Freundlich and Dubinin-Redushkevich models (Freundlich, 1906; Langmuir, 1918; Dubinin et al., 1947) were adopted and can be illustrated as follows:

$$\text{Langmuir: } \frac{1}{q_e} = \frac{1}{Q_o} + \frac{1}{bQ_o} \quad (13)$$

where,  $C_e$  is the equilibrium concentration of phenolics (mg/L),  $q_e$  is the amount of phenolics adsorbed on adsorbent (mg/g).  $Q_o$  and  $b$  are the Langmuir constants related to the adsorption capacity (mg/g) and the energy of adsorption (L/g), respectively.

$$\text{Freundlich: } \log q_e = \log K_f + \frac{1}{n} \log C_e \quad (14)$$

$K_f$  and  $n$  are the Freundlich constants.

$$\text{Dubinin-Redushkevich: } \log q_e = \log q_D - 2B_D R^2 T^2 \log\left(1 + \frac{1}{C_e}\right) \quad (15)$$

$B_D$  is the constant related to the adsorption energy.  $q_D$  is the theoretical saturation capacity (mg/g).  $R$  is the gas constant (J/molK).  $T$  is absolute temperature (K).

The corresponding parameters and regression coefficients ( $R^2$ ) for all phenolics were derived from the individual isotherm models and outcomes are reported in Table 4. Irrespective of adsorbate types, the high value of  $R^2$  ( $>0.99$ ) for Langmuir model as tabulated in Table 4 reveals its applicability for the studied MNPSD-phenolics system. Langmuir plots are hence depicted in Figure 7c, d. From such observation, it can be inferred that phenolics form a monolayer on the MNPSD surface. The maximum monolayer uptake capacity ( $Q_0$ ) of MNPSD for Catechol and Resorcinol was 133.2 and 110.5 mg/g respectively, as calculated from the Langmuir isotherm at 25°C.

From the results of D-R isotherm model that have been shown in Table 4 further reveal that the binding of Catechol and Resorcinol to be a physical process ( $E_D < 8\text{kJ/mol}$ ).

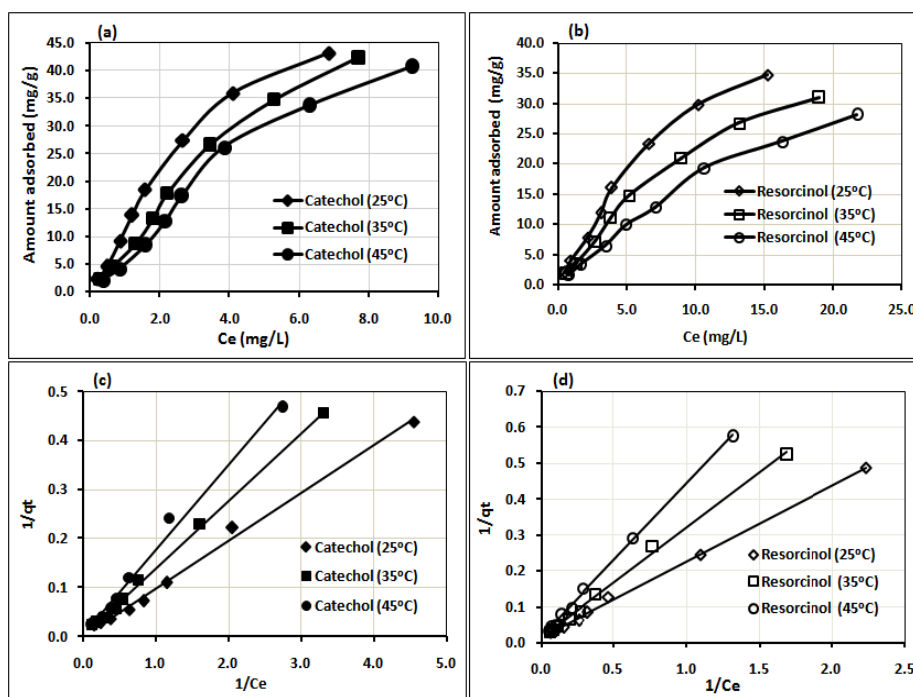


**Figure 7. Isotherm plots for (a) MNPSD-catechol (b) MNPSD-resorcinol at different temperatures applicability of Langmuir model for (c) MNPSD-catechol (d) MNPSD-resorcinol**

**Table 4. Isotherm model parameters for the uptake of catechol and resorcinol onto MNPSD**

Adsorbent	MNPSD					
Temperature	25°C	35°C	45°C	25°C	35°C	45°C
<b>Langmuir model</b>						
Q <sub>o</sub>	133.3	119.1	100.0	110.0	66.7	62.5
b	0.08	0.061	0.058	0.05	0.05	0.04
R <sup>2</sup>	0.99	0.99	0.99	0.99	0.99	0.99
<b>Freundlich model</b>						
K <sub>f</sub>	7.5	5.1	3.2	4.3	3.8	2.5
n	1.38	1.25	1.19	1.20	1.13	1.07
R <sup>2</sup>	0.97	0.97	0.96	0.96	0.98	0.97
<b>Dubinin-Redushkevich model</b>						
q <sub>D</sub>	48.7	42.9	40.3	30.4	26.8	23.3
E <sub>D</sub>	1.78	1.67	1.58	1.56	1.44	1.43
R <sup>2</sup>	0.94	0.95	0.93	0.97	0.93	0.92

#### 4. Conclusion

In the present study, magnetic nanoparticle of sawdust (MNPSD) was investigated a potential Nano adsorbent for sequestration of Catechol and Resorcinol from wastewater. Batch sorption studies revealed that the maximum uptake of Catechol and Resorcinol was achieved at a contact time of 60mins, temperature of 25°C and at low pH of 3. Results, as obtained under batch mode, showed its higher affinity to adsorb Catechol in comparison to Resorcinol could be attributed to its higher log  $k_{ow}$  value and lower solubility in water. Irrespective of adsorbate types, the data as obtained from isotherm studies illustrate that the Langmuir model was more applicable for studied MNPSD-phenolics system. The maximum removal capacities (mg/g) were 133.2mg/g for Catechol and 110.5mg/g for Resorcinol, respectively. Kinetic studies demonstrate that the uptake of such phenolics onto MNPSD followed pseudo-second-order model. Thus, the experimental results reveal the potential application of MNPSD as an effective and suitable Nano adsorbent for remediation of wastewater.

#### Acknowledgement

Authors are grateful to Graphic Era (deemed to be University), Dehradun, India, for giving necessary facilities for the experimental work.

#### References

- Ahmad, T., & Danish, M. (2018). Prospects of banana waste utilization in wastewater treatment: a review. *Journal of Environmental Management*, 206, 330-348.
- Agarwal, S., & Rani, A. (2017). Adsorption of resorcinol from aqueous solution onto CTAB/NaOH/flyash composites: equilibrium, kinetics and thermodynamics. *Journal of Environmental Chemical Engineering*, 5(1), 526-538.
- Akar, T., Ozcan, A. S., Tunali, S., & Ozcan, A. (2008). Biosorption of a textile dye (Acid Blue 40) by cone biomass of thuja oriental is: estimation of equilibrium, thermodynamic and kinetic parameters. *Bio Resource Technology*, 99(8), 3057-3065.
- Bayat, M., Beyki, M. H., & Shemirani, F. (2015). One-step and biogenic synthesis of magnetic Fe<sub>3</sub>O<sub>4</sub>-Fir sawdust composite: Application for selective preconcentration and determination of gold ions. *Journal of Industrial and Engineering Chemistry*, 21, 912-919.

- Chen, X., Xu, R., Xu, Y., Hu, H., Pan, S., & Pan, H. (2018). Natural adsorbent based on sawdust for removing impurities in waste lubricants. *Journal of Hazardous Materials*, 350, 38-45.
- Cui, Y., Masud, A., Aich, N., & Atkinson, J. D. (2019). Phenol and Cr (VI) removal using materials derived from harmful algal bloom biomass: Characterization and performance assessment for a bio sorbent, a porous carbon, and Fe/C composites. *Journal of Hazardous Materials*, 368, 477-486.
- Dubinina, M. M., Zaverina, E. D., & Radushkevich, L. V. (1947). Sorption and structure of active carbons. I adsorption of organic vapors. *Zhurnal Fizicheskoi Khimii*, 21(3), 151-162.
- Freundlich, M. F. (1906). Over the Adsorption in Solution. *The Journal of Physical Chemistry*, 57(1), 385-471.
- Gracioso, L. H., Vieira, P. B., Baltazar, M. P., Avanzi, I. R., Karolski, B., Nascimento, C. A., & Perpetuo, E. A. (2019). Removal of phenolic compounds from raw industrial wastewater by achromobacter sp. isolated from a hydrocarbon-contaminated area. *Water and Environment Journal*, 33(1), 40-50.
- Gupta, V. K., Nayak, A., & Agarwal, S. (2015). Bioadsorbents for remediation of heavy metals: current status and their future prospects. *Environmental Engineering Research*, 20(1), 1-18.
- Gupta, V. K., & Nayak, A. (2012). Cadmium removal and recovery from aqueous solutions by novel adsorbents prepared from orange peel and Fe<sub>2</sub>O<sub>3</sub> nanoparticles. *Chemical Engineering Journal*, 180, 81-90.
- Ho, Y. S., & McKay, G. (1998). A comparison of chemisorption kinetic models applied to pollutant removal on various sorbents. *Process Safety and Environmental Protection*, 76(4), 332-340.
- Ho, Y. S., Ng, J. C. Y., & McKay, G. (2001). Removal of lead (II) from effluents by sorption on peat using second-order kinetics. *Separation Science and Technology*, 36(2), 241-261.
- Issabayeva, G., Hang, S. Y., Wong, M. C., & Aroua, M. K. (2018). A review on the adsorption of phenols from wastewater onto diverse groups of adsorbents. *Reviews in Chemical Engineering*, 34(6), 855-873.
- Jain, M., Yadav, M., Kohout, T., Lahtinen, M., Garg, V. K., & Sillanpaa, M. (2018). Development of iron oxide/activated carbon nanoparticle composite for the removal of Cr (VI), Cu (II) and Cd (II) ions from aqueous solution. *Water Resources and Industry*, 20, 54-74.
- Kurnik, K., Treder, K., Skorupa-Kłaput, M., Tretyn, A., & Tyburski, J. (2015). Removal of phenol from synthetic and industrial wastewater by potato pulp peroxidases. *Water, Air, and Soil Pollution*, 226(8), 254-272.
- Kumar, S., Zafar, M., Prajapati, J. K., Kumar, S., & Kannepalli, S. (2011). Modeling studies on simultaneous adsorption of phenol and resorcinol onto granular activated carbon from simulated aqueous solution. *Journal of Hazardous Materials*, 185(1), 287-294.
- Kataria, N., & Garg, V. K. (2018). Green synthesis of Fe<sub>3</sub>O<sub>4</sub> nanoparticles loaded sawdust carbon for cadmium (II) removal from water: regeneration and mechanism. *Chemosphere*, 208, 818-828.
- Lin, J., Zhan, Y., Zhu, Z., & Xing, Y. (2011). Adsorption of tannic acid from aqueous solution onto surfactant-modified zeolite. *Journal of Hazardous Materials*, 193, 102-111.
- Langmuir, I. (1918). The adsorption of gases on plane surfaces of glass, mica and platinum. *Journal of the American Chemical Society*, 40(9), 1361-1403.
- Mu'azu, N., Jarrah, N., Zubair, M., & Alagha, O. (2017). Removal of phenolic compounds from water using sewage sludge-based activated carbon adsorption: a review. *International Journal of Environmental Research and Public Health*, 14(10), 1-33.
- Mittal, A., Kaur, D., Malviya, A., Mittal, J., & Gupta, V. K. (2009). Adsorption studies on the removal of coloring agent phenol red from wastewater using waste materials as adsorbents. *Journal of Colloid and Interface Science*, 337(2), 345-354.

- Nayak, A., Bhushan, B., Gupta, V., & Sharma, P. (2017). Chemically activated carbon from lignocellulosic wastes for heavy metal wastewater remediation: Effect of activation conditions. *Journal of Colloid and Interface Science*, 493, 228-240.
- Nono, P. N., Kamgaing, T., Raoul, D., Tchuifon, T., & Gabche, S. A. (2016). Optimization of catechol removal from aqueous solution by adsorption on activated carbon from corn cobs and coffee husk. *Chemical Science Transactions*, 5(3), 661-673.
- Sharma, M., Hazra, S., & Basu, S. (2017). Kinetic and isotherm studies on adsorption of toxic pollutants using porous ZnO@ SiO<sub>2</sub> monolith. *Journal of Colloid and Interface Science*, 504, 669-679.
- Soares, P. I., Machado, D., Laia, C., Pereira, L. C., Coutinho, J. T., Ferreira, I. M., Novo, C. M., & Borges, J. P. (2016). Thermal and magnetic properties of chitosan-iron oxide nanoparticles. *Carbohydrate Polymers*, 149, 382-390.
- Suresh, S., Srivastava, V. C., & Mishra, I. M. (2011). Study of catechol and resorcinol adsorption mechanism through granular activated carbon characterization, pH and kinetic study. *Separation Science and Technology*, 46(11), 1750-1766.
- Shakir, K., Ghoneimy, H. F., Elkafrawy, A. F., Beheir, S. G., & Refaat, M. (2008). Removal of catechol from aqueous solutions by adsorption onto organophilic-bentonite. *Journal of Hazardous Materials*, 150(3), 765-773.
- Sun, Y., Chen, J., Li, A., Liu, F., & Zhang, Q. (2005). Adsorption of resorcinol and catechol from aqueous solution by aminated hypercross linked polymers. *Reactive and Functional Polymers*, 64(2), 63-73.
- Villegas, L. G. C., Mashhadi, N., Chen, M., Mukherjee, D., Taylor, K. E., & Biswas, N. (2016). A short review of techniques for phenol removal from wastewater. *Current Pollution Reports*, 2(3), 157-167.
- Weber, W. J., & Morris, J. C. (1963). Kinetics of adsorption on carbon from solution. *Journal of the Sanitary Engineering Division*, 89(2), 31-60.
- Zhao, S., Chen, D., Wei, F., Chen, N., Liang, Z., & Luo, Y. (2017). Removal of Congo red dye from aqueous solution with nickel-based metal-organic framework/graphene oxide composites prepared by ultrasonic wave-assisted ball milling. *Ultrasonics Sonochemistry*, 39, 845-852.
- Zhu, N., Ji, H., Yu, P., Niu, J., Farooq, M., Akram, M., Udego, I. O., Li, H., & Niu, X. (2018). Surface modification of magnetic iron oxide nanoparticles. *Nanomaterials*, 8(10), 810-826.